Synthetic μO-Conotoxin MrVIB Blocks TTX-Resistant Sodium Channel $Na_V1.8$ and Has a Long-Lasting Analgesic Activity†

Grzegorz Bulaj,*,‡,§ Min-Min Zhang,‡ Brad R. Green,‡ Brian Fiedler,‡ Richard T. Layer,§ Sue Wei,§ Jacob S. Nielsen,§ Scott J. Low,§ Brian D. Klein,§ John D. Wagstaff,§ Linda Chicoine,§ T. Patrick Harty,§ Heinrich Terlau,|| Doju Yoshikami,‡ and Baldomero M. Olivera‡

Department of Biology, The University of Utah, Salt Lake City, Utah 84112, Cognetix, Inc., 421 Wakara Way, Salt Lake City, Utah 84108, and Molecular and Cellular Neuropharmacology Group, Max Plank Institute for Experimental Medicine, Goettingen, Germany

Received January 24, 2006; Revised Manuscript Received April 17, 2006

ABSTRACT: μO-Conotoxin MrVIB is a blocker of voltage-gated sodium channels, including TTX-sensitive and -resistant subtypes. A comprehensive characterization of this peptide has been hampered by the lack of sufficient synthetic material. Here, we describe the successful chemical synthesis and oxidative folding of MrVIB that has made an investigation of the pharmacological properties and therapeutic potential of the peptide feasible. We show for the first time that synthetic MrVIB blocks rat $Na_V1.8$ sodium channels and has potent and long-lasting local anesthetic effects when tested in two pain assays in rats. Furthermore, MrVIB can block propagation of action potentials in A- and C-fibers in sciatic nerve as well as skeletal muscle in isolated preparations from rat. Our work provides the first example of analgesia produced by a conotoxin that blocks sodium channels. The emerging diversity of antinociceptive mechanisms targeted by different classes of conotoxins is discussed.

Numerous efforts have focused on the discovery of novel antagonists of sodium channels, in particular, for subtypes resistant to the classical inhibitor of Na channels, tetrodotoxin (*1*, *2*). These channels include the $Na_v1.8$ and -1.9 subtypes that mediate nociceptive signals in dorsal root ganglion (DRG)[1] neurons, making them potential therapeutic targets for the treatment of neuropathic pain. TTX-resistant sodium channels are antagonized by several drugs, including lidocaine, that are used to treat neuropathic pain (*3*−*5*) as well as by other compounds such as ambroxol (*6*) and ketamine (*7*).

The conotoxins produced by venomous cone snails comprise a rich pharmacopoeia of diverse ligands that target sodium channels (*8*, *9*). Two conotoxin families, namely, the μO- and μ-conotoxins, are sodium channel antagonists, whereas δ-conotoxins, such as TxVIA, PVIE, and SVIE, inhibit Na channel inactivation (*10*−*17*). μ-Conotoxins target site I on sodium channels; several were shown to be selective for skeletal muscle subtypes (GIIIA−GIIIC). Recently, small μ-conotoxins were shown to preferentially target TTX-resistant sodium currents in amphibian systems (KIIIA and SIIIA), while some μ-conotoxins exhibited broader targeting specificity (PIIIA or SmIIIA). Table 1 summarizes the structural differences between μO- and μ-conotoxins targeting TTX-resistant sodium channels.

Since the original discovery and preliminary characterization of μO-conotoxins MrVIA and MrVIB a decade ago (*18*, *19*), relatively little progress has been made in studying this group of conotoxins (*20*, *21*). These 31-amino acid peptides contain a large number of nonpolar residues and three disulfide bridges that stabilize the native conformation. MrVIA and MrVIB are highly homologous, differing only in three amino acid positions (Table 1). Recently, native μO-MrVIA and μO-MrVIB isolated from the venom of *Conus marmoreus* were shown to block TTX-resistant Na currents in rat DRG neurons (*20*); MrVIA blocked TTX-resistant currents with an approximately 10-fold higher potency than TTX-sensitive currents. The same work described the NMR structure of the native conotoxin MrVIB, confirming the inhibitory cystine knot (ICK) topology of the disulfide bridges; the authors noted that the lack of efficient synthetic methods precluded further characterization of μO-conotoxins.

In this report, the efficient chemical synthesis and oxidative folding of MrVIB are described in detail. After a two-step, cosolvent-assisted oxidative folding had been optimized, milligram quantities of synthetic MrVIB were produced. The synthetic MrVIB potently inhibited TTX-resistant sodium channels in DRG neurons, as well as cloned rat $Na_V1.8$ channels expressed in oocytes. Its antinociceptive activity

† This work was in part supported by NIH Program Project GM-49677 (to B.M.O. and D.Y.).

* To whom correspondence should be addressed: Department of Biology, The University of Utah, 257 S. 1400 East, Salt Lake City, UT 84112. Phone: (801) 581-8370. Fax: (801) 585-5010. E-mail: bulaj@biology.utah.edu.

‡ The University of Utah.

§ Cognetix, Inc.

|| Max Plank Institute for Experimental Medicine.

[1] Abbreviations: ACN, acetonitrile; BSA, bovine serum albumin; CAP, compound action potential; DMF, dimethylformamide; DRG, dorsal root ganglia; Fmoc, 9-fluorenylmethoxycarbonyl; GSH, reduced glutathione; GSSG, oxidized glutathione; HPLC, high-pressure liquid chromatography; KIIIA, μ-conotoxin KIIIA; MTBE, methyl *tert*-butyl ether; MALDI-TOF, matrix-assisted laser desorption ionization time-of-flight; MrVIB, μO-conotoxin MrVIB; NMP, *N*-methylpyrrolidinone; SIIIA, μ-conotoxin SIIIA; SmIIIA, μ-conotoxin SmIIIA; TCEP, tris-(2-carboxyethyl)phosphine; TFA, trifluoroacetic acid; TTX, tetrodotoxin; VGSCs, voltage-gated sodium channels.

10.1021/bi060159+ CCC: $33.50 © 2006 American Chemical Society
Published on Web 05/20/2006

Table 1: Structures of Conotoxins that Block TTX-Resistant Sodium Channels[a]

Peptide	Sequence	*Conus* species	Ref
μO-conotoxins			
MrVIA	A**C**RKKWEY**C**IVPIIGFIY**CC**PGLI**C**GPFV**C**V	*C. marmoreus*	(*19*)
MrVIB	A**C**SKKWEY**C**IVPILGFVY**CC**PGLI**C**GPFV**C**V	*C. marmoreus*	(*19*)
μ-Conotoxins			
SmIIIA	Z**CC**NGRRG**C**SSRW**C**RDHSR**CC**#	*C. stercusmuscarum*	(*31*)
SIIIA	Z**CC**NG--G**C**SSKW**C**RDHAR**CC**#	*C. striatus*	(*32*)
KIIIA	**CC**N----**C**SSKW**C**RDHSR**CC**#	*C. kinoshitai*	(*32*)

[a] Z is pyroglutamate; # denotes amidated C-terminus.

was tested using both local anesthetic and postincision allodynia assays; in both tests, MrVIB was active and produced antinociceptive effects that lasted up to 24 h. This is the first report of analgesia produced by a conotoxin that blocks sodium channels.

EXPERIMENTAL PROCEDURES

Chemical Synthesis. Conotoxin MrVIB was synthesized on a 357 ACT automatic peptide synthesizer (Advanced ChemTech, Louisville, KY) using Fmoc chemistry on a preloaded Fmoc-Val-Wang or NovaSyn TGA resin (Novabiochem). Orthogonal protection of the Cys pairs included the acid-labile trityl groups (S-Trt) on Cys2, -19, -20, and -30 and the acid-stable *S*-acetamidomethyl groups (*S*-Acm) on Cys9 and Cys25. Side chain protection of non-Cys residues was achieved with *tert*-butyloxycarbonyl (Lys and Trp) and *tert*-butyl (Glu, Ser, and Tyr). To synthesize the peptide on a larger scale, four reaction vessels, each at 750 μM scale, were used. A double-coupling procedure included *N*,*N*′-diisopropylcarbodiimide (DIC) and *N*-hydroxybenzotriazole (HOBt) for 60 min (first coupling), followed by HBTU [2-(1*H*-benzotriazol-1-yl)-1,1,3,3-tetramethyluronium hexafluorophosphate] for 65 min (second coupling). For the last five N-terminal residues, the coupling time was extended to 2 h. Following assembly of the peptide, the N-terminal Fmoc group was removed with 20% piperidine in DMF (dimethylformamide). The peptide was removed from the solid support by a 3 h treatment with reagent K. The peptide was precipitated with cold methyl *tert*-butyl ether (MTBE) chilled to −20 °C. The precipitate was washed four times with cold MTBE. The final precipitate was resuspended in 90% acetonitrile and 0.1% TFA in water, followed by a dilution with a 0.1% TFA/water mixture to a final concentration of 30% acetonitrile. The peptide concentration did not exceed 2 mg/mL. The purification of the linear form was carried out on the same day as the cleavage. A reversed-phase HPLC purification was performed using a preparative diphenyl column (Vydac, model 219TP510) eluted with a linear gradient of acetonitrile in 0.1% TFA in water, changing from 30 to 90% of 90% acetonitrile in the 0.1% TFA/water mixture. The flow rate was 12 mL/min, and the elution was monitored by measuring the absorbance at 220 nm. Approximately 20−30 mg of peptide was applied to the column per run. The collected fractions containing the reduced peptide with a purity of >90% were pooled, frozen at −80 °C, and lyophilized.

Oxidative Folding. The lyophilized reduced MrVIB was resuspended in 90% acetonitrile and the 0.1% TFA/water mixture to yield a 400 μM peptide solution, followed by a 2-fold dilution with the 0.1% TFA/water mixture. The first oxidation step was carried out by mixing the following reaction components (final concentrations in parentheses): 2-propanol (30%), water, Tris-HCl buffer (100 mM, pH 8.7), EDTA (1 mM), GSSG (1 mM), and GSH (2 mM). This mixture was stirred slowly with a magnetic stirrer while the peptide solution was slowly added to a final concentration of 20 μM. The slow stirring of the folding solution continued for 1 h at room temperature (23−25 °C). If any visible precipitation occurred, up to 5% acetonitrile (v/v) was added to the folding solution. The reaction was quenched with formic acid (final concentration of 1%), and the mixture was diluted 2-fold with 0.1% TFA and applied to a preparative diphenyl HPLC column at a flow rate of 5 mL/min. No more than 10 mg of peptide was applied to the column in a given run. Identical HPLC conditions, as described for the purification of the reduced form, were also applied to purify the folding intermediates. The fractions containing the correctly folded isomer were pooled and stored at 4 °C overnight. To monitor folding reactions, C_{18} reversed-phase analytical HPLC separations were carried out in a linear gradient of acetonitrile in 0.1% TFA in water, changing from 25 to 75% of 90% acetonitrile in the 0.1% TFA/water mixture over 25 min.

The second folding step involved formation of the disulfide bond between Cys9 and Cys25 and was carried out at a peptide concentration of 50 μM in 40% acetonitrile, 1 mM iodine, and 2.5% TFA for 20 min at room temperature. The reaction was quenched by adding ascorbic acid until the color disappeared, followed by a 2-fold dilution of the mixture with 0.1% TFA. The oxidation product was purified on the diphenyl preparative HPLC column, as described for the linear form. The fractions containing the correctly folded MrVIB were pooled, and the peptide concentration was determined by measuring the UV absorbance at 280 nm using a calculated molar absorbance coefficient, ϵ, of 8400. The peptide was aliquoted and dried in a Speedvac.

Tests To Compare the Identity of the Synthetic and Native MrVIB. The identity of the folded MrVIB was first confirmed using HPLC coelution experiments with the native peptide. The latter was purified from the venom of *C. marmoreus*, as previously described (*19*). The HPLC analyses were carried out using C_{18} (Vydac 218TP54) and diphenyl (Vydac

219TP54) columns. For the coelution experiments, a gradient of acetonitrile was as follows: from 5 to 55% of 90% acetonitrile in the 0.1% TFA/water mixture over 15 min and then from 55 to 70% over 45 min. The flow rate was 1 mL/min, and the elution was monitored by measuring the absorbance at 220 nm.

In the second analytical test, the disulfide fingerprints of the synthetic and native peptides were compared. The disulfide fingerprints were generated by a mild acidic reduction of the peptides using tris(2-carboxyethyl)phosphine (TCEP), as described in ref *22*. Two nanomoles of synthetic MrVIB was resuspended in 100 μL of 0.2 M sodium citrate buffer (pH 3.0) containing 20 mM TCEP and 6 M guanidinium hydrochloride. The mixture was incubated at ambient temperature and then injected directly onto a diphenyl analytical HPLC column after a given reaction time. A linear gradient of acetonitrile in 0.1% TFA in water, changing from 40 to 80% of 90% acetonitrile in the 0.1% TFA/water mixture over 40 min, was used. The complete time course of this reaction is provided as Supporting Information. An identical TCEP reduction procedure was used for the native peptide isolated from the venom.

Electrophysiology of Frog DRG Neurons. Acutely dissociated neurons from dorsal root ganglia were obtained from 2.5−3 in. adult frogs (*Rana pipiens*) of either sex as previously described (*23*). Briefly, ganglia were treated with collagenase followed by trypsin. Cells were mechanically dissociated by trituration, washed, suspended in 73% Leibowitz's L15 solution (supplemented with 14 mM glucose, 1 mM $CaC1_2$, 7% fetal bovine serum, and penicillin/streptomycin), and stored at 4 °C.

Neurons were perfused with an extracellular solution containing 117 mM NaCl, 2 mM KCl, 2 mM $MgCl_2$, 2 mM $MnCl_2$, 5 mM HEPES, and 10 mM TEA (pH 7.2). To record TTX-resistant currents, 1 μM TTX was added to the bathing solution. Recording pipets (1.5−2 MΩ) contained 10 mM NaCl, 110 mM CsCl, 2 mM $MgCl_2$, 0.4 mM $CaCl_2$, 4.4 mM EGTA, 5 mM HEPES, 5 mM TEA, and 4 mM Na_2ATP (pH 7.2). These solutions inhibit voltage-gated potassium and calcium currents and thereby permit recording of sodium currents alone. Neurons were voltage clamped in the whole-cell configuration, held at −80 mV, and VGSCs were activated by a 50 ms step to 0 mV (for dose−response curves) or steps ranging from −80 to 60 mV (for *I*−*V* curves), applied every 20 s. Each test pulse was preceded by a −120 mV prepulse lasting 50 ms. Current signals, acquired with a MultiClamp 700A amplifier (Axon Instruments, Union City, CA), were filtered at 3 kHz, digitized at 10 kHz, and leak-subtracted by a P/6 protocol using in-house software written in LabVIEW (National Instruments, Austin, TX). Conopeptide MrVIB was freshly dissolved in an extracellular solution containing 1 μM TTX and 0.1% bovine serum albumin (BSA) and applied to neurons being studied by bath exchange. Toxin exposures were conducted in a static bath, and dose−response and *I*−*V* data were obtained after responses had reached a steady state following toxin application.

Electrophysiology of Rat DRG Neurons. To test TTX-resistant (TTX-r) sodium currents in a mammalian system, cells were cultured from dorsal root ganglia (DRG) obtained from postnatal day 9 rat pups. Following dissection, tissue was incubated in an enzyme solution containing a combination of papain, trypsin, and collagenase at 37 °C for 40 min, triturated, and plated on coverslips coated with polyornithine and poly-D-lysine. Cultures were then placed in a CO_2 incubator at 37 °C in a culture medium consisting of DMEM/F12 supplemented with fetal bovine serum, B-27, penicillin and streptomycin, and nerve growth factor (N2).

Cells on coverslips were placed in a recording chamber and perfused at a rate of 0.5−1 mL/min with an extracellular recording solution containing 140 mM NaCl, 3 mM KCl, 1 mM $CaCl_2$, 1 mM $MgCl_2$, 10 mM glucose, and 0.001 mM TTX, 10 mM HEPES, NaOH (pH 7.4). The perfusion system consisted of eight gravity-fed valves operated by a valve controller (Valvelink 16, Automate) that could be triggered from the data collection software (pClamp8, Axon Instruments). For whole-cell recording, electrodes were pulled from borosilicate glass capillary tubing (Warner, GC150TF-10), fire-polished, and filled with an intracellular recording solution containing 140 mM CsF, 10 mM NaCl, 1 mM EGTA, and 10 mM HEPES (pH 7.4) with CsOH. Whole-cell voltage clamp recordings were obtained with a patch clamp amplifier (Axopatch 200B, Axon Instruments) and collected with a PC-based data hardware and software collection package. Data were filtered at 2 kHz, digitized at 20 kHz (Digidata 1200A), and analyzed with pClamp version 8.0. For analysis of TTX-r sodium currents, cells were held at −70 mV and stimulated with voltage-step protocols designed to characterize properties of activation, inactivation, and recovery from inactivation (at this holding potential, most $Na_V1.9$ sodium channels are inactivated and the resulting TTX-r currents represent predominantly $Na_V1.8$ channels). From the activation protocol, the voltage step producing the maximum inward current was used to continuously activate the cell at a rate of 0.1 Hz. After a steady baseline response had been established, the valve controller was used to switch the source of bath perfusion. The delay between switching valves and a change in peak inward current (when observed) varied from 0.5 to 1 min. After a new stable response had been established, the source of perfusion was then switched to a valve containing the next higher concentration in the dose−response analysis or to the control extracellular recording solution after the highest concentration was applied.

To generate inhibitory dose−response relationships, responses obtained in the presence of a given concentration of antagonist were allowed to stabilize, indicating that the bath had reached the desired concentration. Three responses immediately preceding the next concentration change were averaged, plotted as a function of antagonist concentration, and fit with the following logistic equation:

$$I = I_{min} + (I_{max} - I_{min})/[1 + ([L]/IC_{50})^h]$$

where I is the average response amplitude at ligand concentration [L], I_{min} and I_{max} are the response amplitudes at 100% block and in the absence of block, respectively, IC_{50} is the ligand concentration producing 50% inhibition, and h is the Hill coefficient. Typically, all four parameters (I_{min}, I_{max}, IC_{50}, and h) were permitted to vary during the fitting procedure, which involved minimizing the least mean square error using a simplex algorithm (Origin 6.0, Microcal).

Electrophysiology of Rat Sciatic Nerve and Skeletal Muscle Preparations. Sciatic nerves and diaphragm muscles were dissected from adult Sprague-Dawley rats. Before being

used, the sciatic nerve was desheathed and the muscle was cut longitudinally into ~1 mm strips. Compound action potentials (CAPs) were recorded as previously described for frog sciatic nerves and skeletal muscles (*23*). Briefly, the recording chamber was made from a Sylgard (Dow Chemical, Midland, MI) wafer with a linear array of circular wells punched in it. Each well was 4 mm wide and 4 mm deep (50 μL volume) and separated from its neighboring well by a 1 mm partition. The muscle chamber had three such wells and the nerve four. Each preparation was stretched across the wells with one end of the preparation pinned to the floor of the first well and the other end pinned to the floor of the last well (i.e., third well for muscle and fourth for nerve). Portions of the nerve or muscle overlying the partitions between wells were covered with Vaseline. All wells were filled with mammalian Ringer's solution consisting of 140 mM NaCl, 5 mM KCl, 1.1 mM $MgCl_2$, 2 mM $CaCl_2$, and 5 mM HEPES (pH 7.4). Segments of the preparation in a nonend well were held below the meniscus by a pin overlying the tissue and stuck horizontally into the wall of the well. Each compartment was maintained as a static bath, and its fluid contents were refreshed by manual exchange every 15−30 min. Extracellular stimulating electrodes were placed in the first and second wells, and the latter also contained a ground electrode. Extracellular recording electrodes were placed in the third and fourth wells for nerve and second and third wells for muscle. Supra maximal stimuli (~5 V × 0.1 ms, for muscle; ~10 V × 1 ms, for nerve) were applied once per minute to evoke CAPs. CAPs, recorded with a P-55 differential AC amplifier (Grass-Telefactor, West Warrick, RI), were band-pass filtered (1 Hz to 1 kHz) and digitized (4 kHz sampling frequency) using in-house software written in LabVIEW. All electrodes were stainless steel wires. MrVIB was dissolved in mammalian Ringer's solution containing 0.1% BSA and applied to the third well of the nerve preparation or the second well of the muscle preparation.

Electrophysiology of Oocytes. The α-subunit of the rat $Na_v1.8$ channel (NM017247) and the rat Na channel β1-subunit (M91808) were generous gifts from J. Wood (London, U.K.) and from T. Zimmer (Jena, Germany), respectively. Both subunits were expressed in *Xenopus* oocytes as described previously (*24*). Whole-cell currents were recorded under two-electrode voltage clamp control using a Turbo-Tec amplifier (NPI Instruments, Tamm, Germany). The intracellular electrodes were filled with 2 M KCl and had a resistance between 0.5 and 1 MΩ. Currents were low-pass filtered at 3 kHz (−3 dB) and sampled at 10 kHz. The bath solution was normal frog Ringer's solution containing 115 mM NaCl, 2.5 mM KCl, 1.8 mM $CaCl_2$, and HEPES (pH 7.2) (NaOH). Toxin-containing solutions were directly applied to the bath by using a Gilson pipet. All electrophysiological measurements where performed at room temperature (19−22 °C).

Antinociception Assays. Male Sprague-Dawley rats (250−300 g, Charles River Laboratories) were housed in a temperature-controlled (23 ± 3 °C) room with a 12 h light−dark cycle with free access to food and water. The local anesthetic test was performed in rats essentially as described in ref *25*. On the day prior to the test day, a patch on the back of the rat was denuded of hair by shaving it with electric clippers followed by treatment with depilatory cream (Nair). On the following day, the denuded patch was intracutaneously injected with 0.1 mL of lidocaine, bupivacaine, MrVIB, or vehicle (phosphate-buffered saline modified with 1% Tween 80). The injection produced a raised wheal on the surface of the skin, which was circled with a felt-tipped pen. Typically, four injections were made on the back of each animal. The stimulus consisted of mild pinpricks with a 26 gauge needle. The response was a localized skin twitch. A unit test consisted of six uniform pinpricks, 3−5 s apart, within the injected area. Unit scores range from 0 (complete anesthesia) to 6 (no anesthesia). For potency experiments, the unit test was repeated at each site at 5 min intervals for 30 min, and unit test scores were summed (with 36 representing no anesthesia to 0 representing complete anesthesia). For duration experiments, unit tests were performed as described over the course of several hours to days.

A rat incisional pain model (*26*) was used to assess the efficacy of local infiltration of MrVIB. Male Sprague-Dawley rats under isoflurane anesthesia were infused with test articles (MrVIB or vehicle composed of 1% DMSO in saline) subcutaneously into the plantar surface of the foot (0.2 mL). Ten minutes later, a 1 cm longitudinal incision was made through the skin and fascia of the plantar surface of the foot starting 0.5 cm from the heel and extending toward the toes. The plantaris muscle was then injected with 0.1 mL of test article. Approximately 2 min later, the muscle was elevated and incised longitudinally, leaving the muscle origin and insertion intact. The skin was then closed with two sutures, and the animals were allowed to recover from the anesthesia. Prior to the foot incision procedure, rats were placed in plexiglass chambers on an elevated wire mesh frame and allowed to habituate for at least 30 min. Mechanical allodynia was assessed with calibrated von Frey filaments using an up−down method described by Chaplan et al. (*27*). Withdrawal responses to mechanical stimulation with von Frey filaments were assessed at the medial side of the wound near the heel. The 50% withdrawal threshold (the amount of pressure required to produce a flinching response) was calculated. At various times after the incision (1, 2, 4, 6, and 24 h), mechanical allodynia was reassessed in the rats.

RESULTS

Chemical Synthesis and Oxidative Folding. For a decade, the major bottleneck in the characterization of two conotoxins, MrVIA and MrVIB, has been the availability of sufficient material. Although chemical synthesis of MrVIB was achieved in the original characterization of these peptides (*19*), relatively low yields and, consequently, small quantities were obtained (0.1 mg). The authors used Fmoc chemistry to assemble the peptide in a two-step oxidation protocol, in which the native Cys pairs were orthogonally protected using Acm and Trt groups.

For the synthesis carried out in this study, the standard Fmoc solid-phase protocols were used. Both the Wang and the NovaSyn TGA resin yielded a comparable quality and quantity of the crude, reduced MrVIB. A single-coupling protocol resulted in a significantly lower quality of the peptide. Adding Triton X-100 to the solvents (1:1 DMP:NMP ratio) did not improve synthesis. Since lower coupling yields were observed after Trp6, the coupling time for each of the last five residues was extended to 2 h. After the

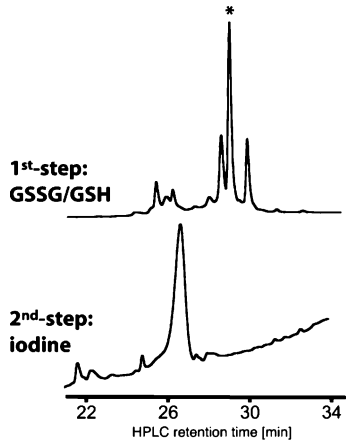

FIGURE 1: HPLC analysis of the oxidative folding of MrVIB. Folding reactions were monitored by reversed-phase HPLC analysis using a diphenyl Vydac column as described in Experimental Procedures. The top trace shows the folding reaction after oxidation for 1 h in the presence of 1 mM GSSG, 2 mM GSH, 30% 2-propanol, and 100 mM Tris-HCl (pH 8.7). The asterisk denotes the main folding product that was subjected to the second oxidation step. The bottom trace shows the folding reaction after incubation for 20 min in the presence of 1 mM iodine, 40% acetonitrile, and 2.5% TFA. The purity of the final oxidation product is shown in Figure 2.

assembly of the peptide, MrVIB was cleaved from the resin and purified by reversed-phase HPLC with an estimated 10% yield using preparative diphenyl columns, rather than more commonly used C_{18}-based columns.

To produce larger quantities of peptides containing more than two disulfide bridges, a single-step oxidation is often preferable. Therefore, our initial efforts were focused on detergent-assisted oxidative folding methods previously used to produce highly hydrophobic conotoxins such as δ-SVIE and δ-PVIA (*15*, *28*). Our experiments indicated that nonionic detergents could indeed improve folding yields of MrVIB (data not shown). However, this approach presented problems during scale-up preparative HPLC separations of the folding mixtures containing the detergent: Tween prevented the peptide from sticking to the column when applied in larger volumes.

A two-step oxidation method that involved orthogonal protection of the Cys pairs and a regioselective formation of disulfide bridges was then employed (*19*, *29*, *30*). Oxidation of four Cys residues results in three isomers, of which only one contained the proper connectivity of the disulfide bonds. To improve the yield of the correct isomer, several folding conditions were tested, including addition of organic cosolvents or nonionic detergents. The presence of higher concentrations of methanol (>30%), 2-propanol (>20%), or 2% Tween 20 detergent significantly improved the relative accumulation of the correct isomer. In scaled-up separations of the folding mixture, the 2-propanol-assisted oxidation protocol proved to be the most efficient. Figure 1 shows the HPLC analysis of the folding mixture from the first and second oxidation steps. After a large-scale purification, the isomer was further oxidized using iodine as described in Experimental Procedures. Extending the oxidation time beyond 20 min resulted in lower yields of recovery of the folded MrVIB. After final HPLC purification, the correctly folded MrVIB was >90% pure, as determined by analytical HPLC using diphenyl and C_{18} Vydac columns

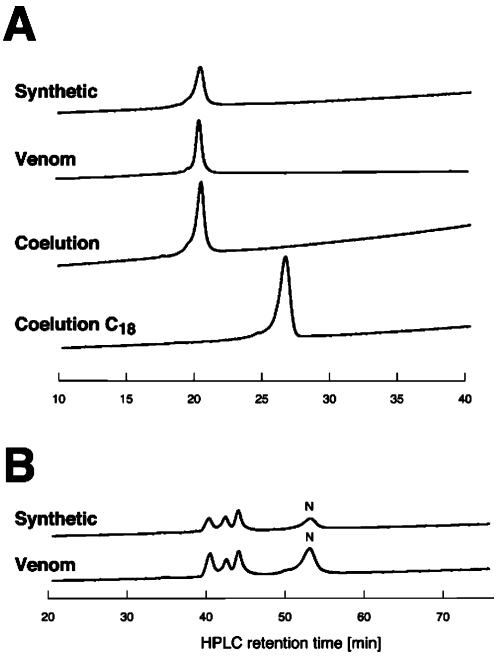

FIGURE 2: Comparison of the synthetic and native MrVIB by HPLC coelution and disulfide fingerprints. (A) HPLC coelution experiments. The first three HPLC traces represent the synthetic, the venom-derived peptide, and a 1:1 mixture of the two peptides (Coelution) analyzed on a diphenyl Vydac HPLC column. The bottom HPLC trace (Coelution C18) represents the same 1:1 mixture, but separated on a C18 Vydac HPLC column. (B) Comparing disulfide fingerprints of the synthetic and the venom-derived MrVIB. Both HPLC traces represent products of a 20 min acidic reduction with 20 mM TCEP in the presence of 6 M guanidinium hydrochloride and 0.2 M sodium acetate buffer (pH 3.0). The reaction solutions were directly injected into a diphenyl HPLC column and eluted in a linear gradient of acetonitrile, as described in Experimental Procedures. N denotes the peak corresponding to the folded MrVIB. The complete time course of the TCEP reduction of the synthetic MrVIB is available as Supporting Information.

(Figure 2A). The peptide had the expected molecular weight, as determined by MALDI-TOF mass spectrometry [MH^+] = 3407.7 (calculated average [MH^+] = 3407.2). Using the protocol described above, several milligrams of MrVIB were produced. The final yield from the purified reduced peptide to the final product was estimated to be approximately 10%.

The solubility of μO-conotoxin MrVIB in aqueous solutions has been a problem in the previous electrophysiological studies. The synthetic peptide could not be efficiently resuspended in water or saline solutions at concentrations of >5 μM. Addition of organic solvent at 20−40% or 1% Tween 80 dramatically improved the solubility of the peptide, making 20−100 μM stock solutions feasible.

Chemical Identity of Synthetic and Native MrVIB. To establish that the synthetic MrVIB was identical to the native peptide (purified from venom), two different analytical methods were employed: HPLC coelution experiments using two different stationary phases and a comparison of disulfide fingerprints. As illustrated in Figure 2A, the synthetic and native peptides had identical HPLC retention times when eluted on a Vydac diphenyl analytical HPLC column. Subsequently, the two peptides were mixed in a 1:1 ratio prior to injection on Vydac diphenyl or C_{18} HPLC columns. The two HPLC coelution experiments yielded a single peak (Figure 2A), indicating that both peptides behaved identically

on the two different stationary phases, consistent with their chemical identity.

The synthetic and native MrVIB were also compared using so-called "disulfide fingerprints" (Figure 2B). Disulfide fingerprints are generated by a partial reduction of disulfide-rich peptides with tris(2-carboxyethyl)phosphine (TCEP), followed by HPLC analysis (*22*). Under acidic conditions (pH 3.0), the peptide disulfide bonds are reduced without the possibility of any intramolecular thiol−disulfide rearrangements (disulfide scrambling). Thus, for the native peptide isolated from the venom, the resulting distribution of partially unfolded species represents only intermediates containing the native disulfide bridges. Comparison of the HPLC elution patterns of the unfolding intermediates (disulfide fingerprints) of the native and synthetic MrVIB thus provides a robust assessment of the identity of their disulfide connectivities.

First, the synthetic MrVIB was subjected to partial TCEP reduction under denaturing conditions (see Experimental Procedures), and the time course of the TCEP reduction was established (see the Supporting Information). Since a 20 min reaction yielded equally distributed unfolding species (disulfide fingerprint), this time point was chosen so the synthetic and native peptides could be compared. Both peptides were subjected to a 20 min TCEP reduction, followed by HPLC analyses. As illustrated in Figure 2B, the disulfide fingerprints generated by the partial reduction of the synthetic and the native MrVIB were identical. Thus, by both HPLC coelution and TCEP fingerprinting, the synthetic and the native MrVIB were indistinguishable.

Electrophysiological Studies. The effect of synthetic MrVIB on TTX-resistant sodium currents in dissociated frog DRG neurons was characterized. Whole-cell recordings from frog DRG neurons showed that MrVIB blocked TTX-resistant currents in these neurons with an IC_{50} of 530 nM (Figure 3). The recovery from block was slow and incomplete even after washing had been carried out for 20 min. Furthermore, the voltage sensitivities of the TTX-resistant current before and during partial block by MrVIB are similar (Figure 4), indicating that the peptide does not affect the gating properties of the TTX-resistant channel. Previously published results which showed that μO-conotoxins potently inhibited TTX-resistant sodium currents in rat DRG neurons (*20*) were confirmed using synthetic MrVIB. Synthetic MrVIB blocked rat DRG neuron TTX-resistant currents with an IC_{50} of 13 nM.

To investigate the biological activity of MrVIB on specific TTX-resistant Na channels, synthetic MrVIB was tested against the cloned rat $Na_V1.8$ subtype of the sodium channel, expressed in the *Xenopus* oocyte system. Two-electrode voltage clamp experiments were performed in the absence and presence of MrVIB; as shown in Figure 5, synthetic MrVIB (0.5 μM) resulted in a profound inhibition of the evoked currents.

To study the effects of MrVIB on the propagation of action potentials, CAPs were recorded from isolated sciatic nerve and skeletal muscle preparations from rat, as described in Experimental Procedures. In the sciatic nerve, two biphasic CAPs were recorded, a fast conduction velocity A-CAP and slower C-CAP, and both were susceptible to MrVIB (Figure 6A). Following exposure to 1 μM MrVIB, >97% of the A-CAP and ~50% of the C-CAP were blocked (Figure 6A,C). The C-CAP that persisted in 1 μM MrVIB had a longer latency, indicating that the toxin slowed the conduction velocity of the action potential in the C-fibers that remained active; furthermore, the C-CAP could be completely blocked within 20 min when the MrVIB concentration was increased to 5 μM (not illustrated). Like A-CAPs in sciatic nerve, action potentials in skeletal muscle were largely blocked by 1 μM MrVIB (Figure 6B), albeit with a slower time course (Figure 6C).

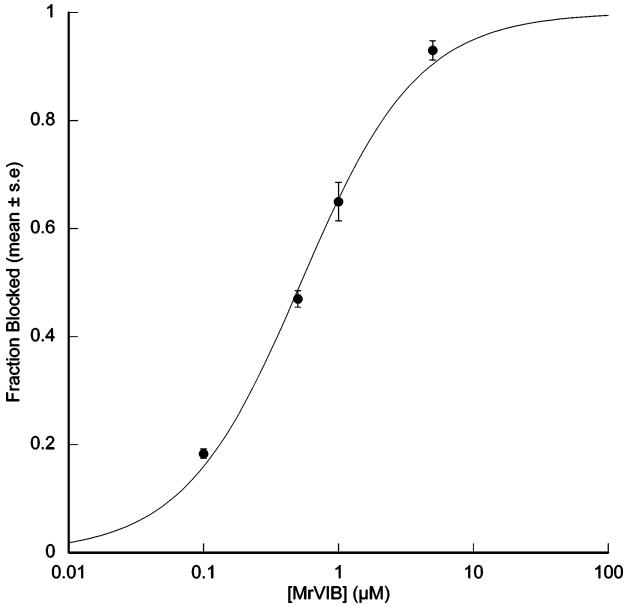

FIGURE 3: Dose-dependent block of TTX-resistant currents in frog DRG neurons by synthetic MrVIB. Sodium currents were acquired as described in Experimental Procedures. The fraction of peak current blocked by MrVIB at steady state is plotted as a function of peptide concentration. The solid line represents the best fit curve to the equation for a rectangular hyperbola, fraction blocked = 1/(1 + IC_{50}/[MrVIB]), with an IC_{50} value of 0.53 μM. N = 3−4 cells for each concentration.

Antinociceptive Tests. To explore the antinociceptive potential of MrVIB, the synthetic peptide was tested using two assays that utilize the response of a rat to a mildly painful stimulus as a reversible end point: local anesthesia and postincision allodynia. The peptide produced a dose-dependent and long-lasting suppression of the skin twitch response in the subcutaneous wheal test in male rats (Figure 7). The ED_{50} for producing a local anesthetic effect (approximately 100 pmol) was at least 2 orders of magnitude lower than that for lidocaine. The duration of action of MrVIB was also much longer than that of lidocaine. Full recovery from the local anesthetic effect of the conotoxin was observed after 24 h (1 nmol dose) and 48 h (10 nmol dose), while with lidocaine, full recovery from the treatment occurred after ~3 h.

Local infusion of MrVIB (30 nmol) into the plantar surface of the foot prior to the incision produced a long-lasting (>6 h) reduction of postincision allodynia in rats (Figure 8). This was manifested as an increase in the withdrawal threshold to mechanical stimulation. Local infiltration of tetracaine (0.5%) produced a modest reduction of allodynia at 1 h which was gone by 2 h postincision. No untoward effects on healing of the incision were noted in rats that were observed for several days after the incision in any treated group.

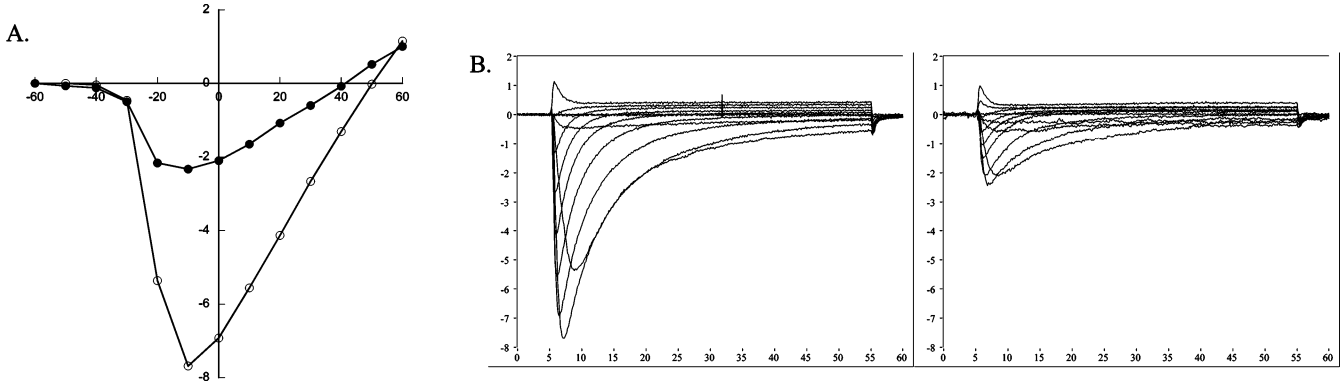

FIGURE 4: MrVIB blocks TTX-resistant sodium currents in frog DRG without affecting its voltage sensitivity. Sodium currents were acquired as described in Experimental Procedures. (A) $I-V$ curves before (○) and during (●) exposure to 1 μM MrVIB. (B) Corresponding current traces before (left) and during (right) exposure to 1 μM MrVIB. TTX (1 μM) was present throughout the experiment.

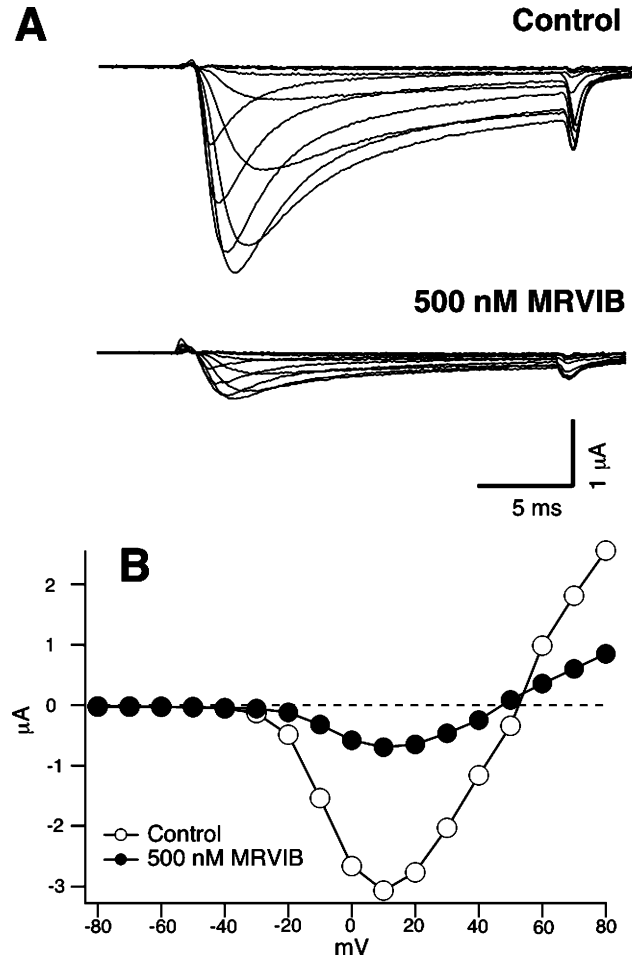

FIGURE 5: MrVIB blocks $Na_V1.8$ channels. (A) Whole-cell currents were recorded from *Xenopus* oocytes expressing $Na_V1.8$ channels as described in Experimental Procedures. Depolarizing pulses from −60 to 40 in 10 mV steps from a holding potential of −100 mV are shown. Addition of 500 nM MrVIB leads to a profound reduction in currents (bottom panel). (B) Comparison of the current−voltage relationship under control conditions and in the presence of 500 nM MrVIB.

DISCUSSION

Conotoxins that act like sodium channel blockers belong to two families, the μO- and μ-conotoxins (Table 1). In contrast to the progress made in the characterization of the μ-conotoxin family (see, for example, refs *23*, *31*, and *32*), μO-conotoxins have not been extensively investigated; this is largely due to the failure to obtain sufficient synthetic material. In this paper, we describe the chemical synthesis and oxidative folding of MrVIB with yields sufficient to allow a much more comprehensive characterization of the pharmacological properties and therapeutic potential of this class of peptides to be feasible.

Our chemical synthesis protocol, including a two-step oxidative folding, produced milligram quantities of MrVIB with a purity exceeding 90% and a final yield of 10%. Although this yield, as calculated from the purified reduced peptide to the final product, may seem rather modest, it represents a major improvement over existing methods for producing such hydrophobic peptides. Our initial attempts to follow the original two-step protocol (*19*) resulted in producing only analytical amounts of the synthetic material with yields significantly lower that 1%. Scaling-up chemical synthesis and oxidative folding of MrVIB presented a major technological challenge, since such a hydrophobic peptide has a strong tendency to aggregate and precipitate at every processing step, including oxidation and HPLC purifications. This challenge is further reflected by a fact that all recent studies with MrVIA and MrVIB, including structural and electrophysiological experiments (*20*) and antinociceptive assays in animal models (*33*), have all been performed with natural toxins isolated from the venom of *C. marmoreus*.

There were several technical improvements over the previous method that made the chemical synthesis of MrVIB more efficient. Adding organic solvents improved folding yields and recovery of the synthetic MrVIB at every processing step. In particular, the cosolvent-assisted folding resulted in an improved accumulation of correctly folded forms (Figure 1). The largest losses of peptide were observed during two preparative HPLC steps: (i) when the reduced peptide was purified from a crude, postcleavage mixture and (ii) during purification of the correctly folded isomer after the first folding step. Two improvements in the preparative purification steps were application of the peptide mixture to an HPLC column equilibrated with a relatively high concentration of organic mobile phase (initial concentration of 27% acetonitrile in the 0.1% TFA/water mixture) and the change from C_{18}- to diphenyl-based reversed-phase columns. The availability of much greater amounts of MrVIB has made it possible to carry out a more extensive pharmacological characterization, including assessment of the activity of the peptide in antinociceptive assays using animal models.

Our pharmacological characterization demonstrated that μO-MrVIB blocked TTX-resistant sodium currents in both

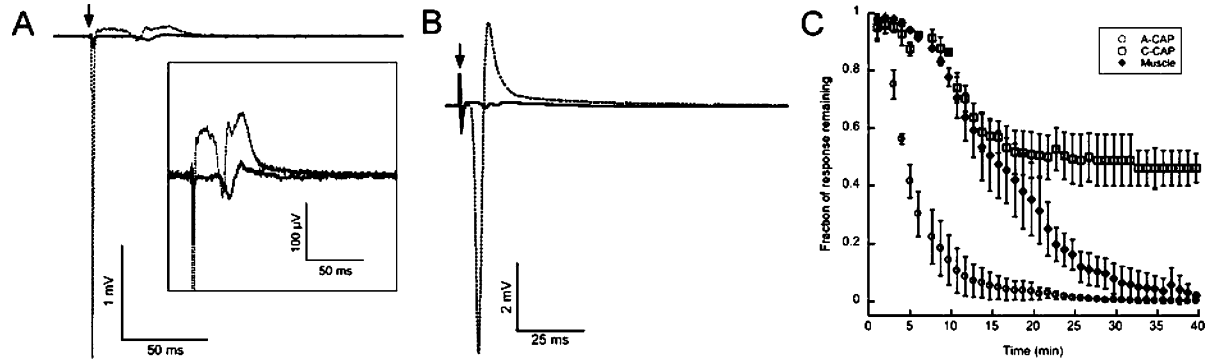

FIGURE 6: MrVIB blocks action potentials in rat sciatic nerve and skeletal muscle. CAPs were recorded as described in Experimental Procedures. Representative recordings that are shown are the average of five responses before (gray dotted traces) and during (solid black traces) exposure to 1 μM MrVIB. (A) Recordings from sciatic nerve. Electrical stimulus, applied at the arrow, evoked a large biphasic fast A-CAP within a millisecond, followed ~30 ms later by a smaller biphasic C-CAP. The A-CAP amplitude (as measured from the baseline to the peak of its negative phase) was blocked by 97% following toxin exposure. The inset shows the same traces with the vertical axis expanded to more clearly show the C-CAP. In the control trace, the C-CAP rides on the second, positive phase of the A-CAP; this phase of the A-CAP was essentially obliterated following MrVIB exposure, leaving behind an attenuated C-CAP whose amplitude (from the peak of its negative phase to the peak of its positive phase) was approximately half of that in the control response. (B) Muscle responses. The stimulus (see the artifact at the arrow) was followed within a few milliseconds by a biphasic CAP whose peak amplitude (from the baseline to the peak of its negative phase) was reduced by 99% after exposure to MrVIB. (C) Time course of block by 1 μM MrVIB of sciatic nerve A-CAP (○) and C-CAP (□) and muscle CAP (◆). MrVIB was applied at time zero. Each point represents the average response (± the standard error of the mean) from three preparations each of nerve and muscle.

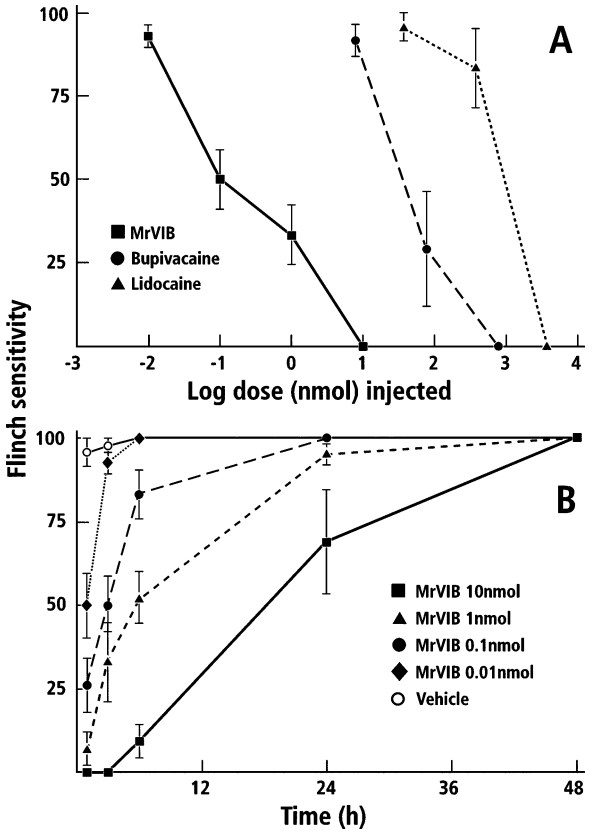

FIGURE 7: Antinociceptive activity of MrVIB conotoxin. (A) MrVIB inhibits skin flinch sensitivity in the rat local anesthetic assay with greater potency than either lidocaine or bupivacaine. Data represent the percentage of flinches observed after six pinpricks (the unit test) at the time of peak effect (the 30 min time point for bupivacaine and lidocaine and the 3 h time point for MRVIB). Each point represents the mean of at least four observations. (B) MrVIB produces a long-lasting inhibition of skin flinch sensitivity in the rat local anesthetic assay. Data represent the percentage of flinches observed of six total at each time point. Each point represents the mean of at least seven observations.

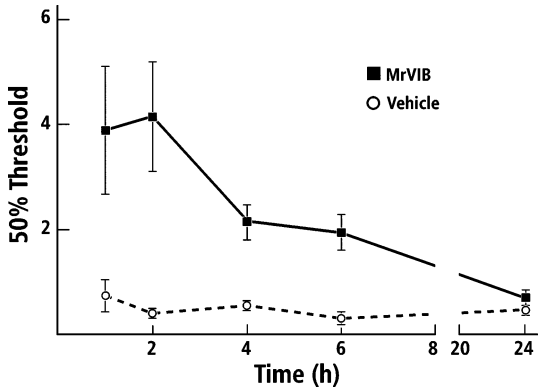

FIGURE 8: MrVIB reduces postincision allodynia following subcutaneous infusion of 30 nmol of the peptide. Data represent the calculated 50% withdrawal threshold at a given test period. Each point represents the mean of five to seven observations.

frog and rat DRG neurons. The dose−response curves for the synthetic MrVIB on rat neurons gave an IC_{50} of ~13 nM, 6-fold lower than the IC_{50} of venom-isolated MrVIA (83 nM) (*20*). The observed difference might be ascribed to either (1) the structural differences between MrVIA and MrVIB (see Table 1) or (2) technical differences in the handling of the peptides. In two previous reports, MrVIA and MrVIB had comparable activities in blocking transient sodium currents in rat DRG neurons (*20*) and potencies in blocking $Na_v1.4$ sodium channels (*34*). However, the latter authors (*34*) observed a significantly different potency of MrVIA in blocking $Na_v1.2$ channels as compared to that published in ref *35*. It is possible that the observed differences in the potency of MrVIB or MrVIA in different laboratories result from solubility problems with μO-conotoxins: these peptides have a tendency to stick to test tubes at lower concentrations and to precipitate at higher concentrations. Thus, the dose−response curves may depend on what solvents and containers are used for resuspension and dilution of the peptides.

We have also directly demonstrated that MrVIB blocks $Na_V1.8$ channels (Figure 5), a subtype of great potential interest in the antinociceptive drug development field. In knockout mouse studies, $Na_V1.8$ was shown to be involved

Table 2: Diversity of Analgesic Conotoxins and Their Molecular Targets[a]

Conotoxin	Structure	Molecular target/mechanism	Reference
ω-MVIIA	CKGKGAKCSRLMYDCCTGSCRSGKC	Voltage-gated calcium channels Antagonist	(*40*)
μO-MrVIB	ACSKKWEYCIVPILGFVYCCPGLICGPFVCV	Voltage-gated sodium channels Antagonist	This work
χ-MrIA	NGVCCGYKLCHOC	Norepinephrine transporter Inhibitor	(*41-43*)
ACV-1 (Vc1.1)	GCCSDPRCNYDHPEIC	Neuronal nicotinic receptors Antagonist	(*44, 45*)
Contulakin-G	ZSEEGGSNATKKPYIL	G-protein coupled receptors Agonist	(*46*)
Conantokin-G	GEγγLQγNQγLIRγKSN	NMDA receptors Antagonist	(*47*)

[a] Z is pyroglutamate; O is hydroxyproline.

in processing pain signals; mice deficient in $Na_V1.8$ were less responsive to noxious mechanical stimuli and demonstrated a delayed development of inflammatory hyperalgesia (*36*).

MrVIB also inhibits TTX-sensitive currents. All reports on the effects of MrVIB on TTX-sensitive currents have yielded IC_{50} values of >200 nM (*20*, *21*, *35*; B. Klein, unpublished data). TTX-sensitive currents also play a critical role in neuropathic pain states since TTX itself reduces mechanical allodynia after nerve injury (*37*). The in vivo effects of MrVIB demonstrated in this study utilized responses to the transmission of acute nociceptive pain in normal animals. Both TTX-resistant and -sensitive sodium channels play a role in the normal transmission of acute pain. The extended duration of the MrVIB activity, coupled with its potency at sodium channels underlying nociception, indicates its potential therapeutic utility in the treatment of pain.

In view of MrVIB's apparent broad selectivity, its effects on the propagation of action potentials in nerve and muscle of rat were examined. Skeletal muscles express (TTX-sensitive) $Na_V1.4$, and as might be expected, the muscle CAP is 99% blocked by 1 μM MrVIB (Figure 6B,C). Sciatic nerve has A-fibers with TTX-sensitive sodium channels as well as C-fibers with both TTX-sensitive and TTX-resistant channels. The corresponding action potentials supported by A- and C-fibers are manifested in extracellular recordings as A- and C-CAPs, respectively. In rat sciatic nerve, TTX readily blocks the A-CAP, and although the C-CAP is also largely blocked by TTX, a minor fraction can persist (*38*; B. Fiedler and D. Yoshikami, unpublished observations). At a concentration of 1 μM, MrVIB blocked essentially all of the A-CAP and approximately half of the C-CAP (Figure 6A,C); the C-CAP that persists has a longer latency (Figure 6A) and can be totally blocked by 5 μM MrVIB (not illustrated). This differential effect on A- versus C-fibers mirrors the effects of local anesthetics on A- and C-fibers in rabbit vagus nerve (*39*).

The synthetic material described above has been used in a collaborative effort with the laboratory of S. Heinemann (Jena, Germany) for a much more thorough biophysical characterization of the effects of MrVIB on neuronal voltage-gated sodium channels (*34*). The data reveal that MrVIB has significant differences in the affinity for various sodium channel subtypes and have unequivocally established that the peptide is not an open channel blocker. Rather, MrVIB appears to act at a unique site in domain III. It is tempting to speculate here that perhaps this unique interaction between MrVIB and the sodium channels may be in part responsible for the long-lasting local anesthetic effect of the conotoxin (shorter-acting lidocaine is known to target the inner vestibule of the channel). The biophysical studies have also clearly differentiated between μ- and μO-conotoxins on the basis of such parameters as changes in the open state probability upon toxin binding. Thus, the availability of substantial amounts of synthetic toxin has already led to mechanistic insights into how MrVIB interacts with its target sodium channels and suggests that MrVIB, which is the first conotoxin with analgesic properties that acts on sodium channels, does so through a unique mechanism.

What is remarkable is the emerging collection of various analgesic conotoxins that act through diverse mechanisms, with none involving opioid receptors. As summarized in Table 2, several conotoxins have potential therapeutic application in pain management, each working through a distinct mechanism. The first analgesic conotoxin, ω-MVIIA, also known as ziconotide or Prialt, was recently approved for treatment of chronic intractable pain in both the United States and Europe. Other conotoxins are currently at various stages of preclinical and clinical development. The work presented here adds one more important example of the

unprecedented analgesic pharmacopoeia that is being provided by *Conus* snails.

SUPPORTING INFORMATION AVAILABLE

One figure illustrating the complete time course of the TCEP reduction of the synthetic MrVIB. This material is available free of charge via the Internet at http://pubs.acs.org.

REFERENCES

1. Black, J. A., Liu, S., Tanaka, M., Cummins, T. R., and Waxman, S. G. (2004) Changes in the expression of tetrodotoxin-sensitive sodium channels within dorsal root ganglia neurons in inflammatory pain, *Pain 108*, 237−47.
2. Wood, J. N., Boorman, J. P., Okuse, K., and Baker, M. D. (2004) Voltage-gated sodium channels and pain pathways, *J. Neurobiol. 61*, 55−71.
3. Brau, M. E., and Elliott, J. R. (1998) Local anaesthetic effects on tetrodotoxin-resistant Na^+ currents in rat dorsal root ganglion neurones, *Eur. J. Anaesthesiol. 15*, 80−8.
4. Brau, M. E., Branitzki, P., Olschewski, A., Vogel, W., and Hempelmann, G. (2000) Block of neuronal tetrodotoxin-resistant Na^+ currents by stereoisomers of piperidine local anesthetics, *Anesth. Analg. 91*, 1499−505.
5. Brau, M. E., Dreimann, M., Olschewski, A., Vogel, W., and Hempelmann, G. (2001) Effect of drugs used for neuropathic pain management on tetrodotoxin-resistant Na^+ currents in rat sensory neurons, *Anesthesiology 94*, 137−44.
6. Weiser, T., and Wilson, N. (2002) Inhibition of tetrodotoxin (TTX)-resistant and TTX-sensitive neuronal Na^+ channels by the secretolytic ambroxol, *Mol. Pharmacol. 62*, 433−8.
7. Zhou, Z. S., and Zhao, Z. Q. (2000) Ketamine blockage of both tetrodotoxin (TTX)-sensitive and TTX-resistant sodium channels of rat dorsal root ganglion neurons, *Brain Res. Bull. 52*, 427−33.
8. Terlau, H., and Olivera, B. M. (2004) *Conus* venoms: A rich source of novel ion channel-targeted peptides, *Physiol. Rev. 84*, 41−68.
9. French, R. J., and Terlau, H. (2004) Sodium channel toxins: Receptor targeting and therapeutic potential, *Curr. Med. Chem. 11*, 3053−64.
10. Fainzilber, M., Kofman, O., Zlotkin, E., and Gordon, D. (1994) A new neurotoxin receptor site on sodium channels is identified by a conotoxin that affects sodium channel inactivation in molluscs and acts as an antagonist in rat brain, *J. Biol. Chem. 269*, 2574−80.
11. Fainzilber, M., Lodder, J. C., Kits, K. S., Kofman, O., Vinnitsky, I., Van Rietschoten, J., Zlotkin, E., and Gordon, D. (1995) A new conotoxin affecting sodium current inactivation interacts with the δ-conotoxin receptor site, *J. Biol. Chem. 270*, 1123−9.
12. Shon, K., Hasson, A., Spira, M. E., Cruz, L. J., Gray, W. R., and Olivera, B. M. (1994) δ-Conotoxin GmVIA, a novel peptide from the venom of *Conus gloriamaris*, *Biochemistry 33*, 11420−5.
13. Shon, K., Grilley, M. M., Marsh, M., Yoshikami, D., Hall, A. R., Kurz, B., Gray, W. R., Imperial, J. S., Hillyard, D. R., and Olivera, B. M. (1995) Purification, characterization and cloning of the lockjaw peptide from *Conus purpurascens* venom, *Biochemistry 34*, 4913−8.
14. Barbier, J., Lamthanh, H., Le Gall, F., Favreau, P., Benoit, E., Chen, H., Gilles, N., Illan, N., Heinemann, S. H., Gordon, D., Menez, A., and Molgo, J. (2004) A δ-conotoxin from *Conus ermineus* venom inhibits inactivation in vertebrate neuronal Na^+ channels but not in skeletal and cardiac muscles, *J. Biol. Chem. 279*, 4680−5.
15. Bulaj, G., DeLa Cruz, R., Azimi-Zonooz, A., West, P., Watkins, M., Yoshikami, D., and Olivera, B. M. (2001) δ-Conotoxin structure/function through a cladistic analysis, *Biochemistry 40*, 13201−8.
16. Leipold, E., Hansel, A., Olivera, B. M., Terlau, H., and Heinemann, S. H. (2005) Molecular interaction of δ-conotoxins with voltage-gated sodium channels, *FEBS Lett. 579*, 3881−4.
17. West, P. J., Bulaj, G., and Yoshikami, D. (2005) Effects of δ-conotoxins PVIA and SVIE on sodium channels in the amphibian sympathetic nervous system, *J. Neurophysiol. 94*, 3916−24.
18. Fainzilber, M., van der Schors, R., Lodder, J. C., Li, K. W., Geraerts, W. P., and Kits, K. S. (1995) New sodium channel blocking conotoxins also affect calcium currents in *Lymnaea* neurons, *Biochemistry 34*, 5364−71.
19. McIntosh, J. M., Hasson, A., Spira, M. E., Gray, W. R., Li, W., Marsh, M., Hillyard, D. R., and Olivera, B. M. (1995) A new family of conotoxins that blocks voltage-gated sodium channels, *J. Biol. Chem. 270*, 16796−802.
20. Daly, N. L., Ekberg, J. A., Thomas, L., Adams, D. J., Lewis, R. J., and Craik, D. J. (2004) Structures of μO-conotoxins from *Conus marmoreus*. Inhibitors of tetrodotoxin (TTX)-sensitive and TTX-resistant sodium channels in mammalian sensory neurons, *J. Biol. Chem. 279*, 25774−82.
21. Terlau, H., Stocker, M., Shon, K. J., McIntosh, J. M., and Olivera, B. M. (1996) μO-Conotoxin MrVIA inhibits mammalian sodium channels but not through site I, *J. Neurosci. 76*, 1423−9.
22. Gray, W. (1997) Disulfide bonds between cysteine residues, in *Protein Structure: A Practical Approach* (Creighton, T., Ed.) pp 165−85, IRL Press, New York.
23. Zhang, M. M., Fiedler, B., Green, B. R., Catlin, P., Watkins, M., Garrett, J. E., Smith, B. J., Yoshikami, D., Olivera, B. M., and Bulaj, G. (2006) Structural and Functional Diversities among μ-Conotoxins Targeting TTX-resistant Sodium Channels, *Biochemistry 45*, 3723−32.
24. Jacobsen, R. B., Koch, E. D., Lang-Malecki, B., Stocker, M., Verhey, J., van Wagoner, R. M., Vyazovkina, A., Olivera, B. M., and Terlau, H. (2000) Single amino acid substitutions in κ-conotoxin PVIIA disrupt interaction with the *Shaker* K^+ channel, *J. Biol. Chem. 275*, 24639−44.
25. Bulbring, W., and Wajda, I. (1945) Biological comparison of local anesthetics, *J. Pharmacol. Exp. Ther. 85*, 78−84.
26. Brennan, T., Vandermeulen, E., and Gebhart, G. (1996) Characterization of a rat model of incisional pain, *Pain 64*, 493−501.
27. Chaplan, S. R., Pogrel, J. W., and Yaksh, T. L. (1994) Role of voltage-dependent calcium channel subtypes in experimental tactile allodynia, *J. Pharmacol. Exp. Ther. 269*, 1117−23.
28. DeLa Cruz, R., Whitby, F. G., Buczek, O., and Bulaj, G. (2003) Detergent-assisted oxidative folding of δ-conotoxins, *J. Pept. Res. 61*, 202−12.
29. Annis, I., Hargittai, B., and Barany, G. (1997) Disulfide bond formation in peptides, *Methods Enzymol. 289*, 198−221.
30. Moroder, L., Besse, D., Musiol, H. J., Rudolph-Bohner, S., and Siedler, F. (1996) Oxidative folding of cystine-rich peptides vs. regioselective cysteine pairing strategies, *Biopolymers 40*, 207−34.
31. West, P. J., Bulaj, G., Garrett, J. E., Olivera, B. M., and Yoshikami, D. (2002) μ-Conotoxin SmIIIA, a potent inhibitor of TTX-resistant sodium channels in amphibian sympathetic and sensory neurons, *Biochemistry 41*, 15388−93.
32. Bulaj, G., West, P. J., Garrett, J. E., Marsh, M., Zhang, M.-M., Norton, R. S., Smith, B. J., Yoshikami, D., and Olivera, B. M. (2005) Novel conotoxins from *Conus striatus* and *Conus kinoshitai* selectively block TTX-resistant sodium channels, *Biochemistry 44*, 7259−65.
33. Aslan, S., Jayamanne, A., Lewis, R. J., Thomas, L., Christie, M. J., Vaughan, C. W., Ekberg, J. A., Adams, D. J., Wood, J. N., and Baker, M. D. (2005) in *Venoms to Drugs 2005*, Heron Island, Australia.
34. Zorn, S., Leipold, E., Hansel, A., Bulaj, G., Olivera, B. M., Terlau, H., and Heinemann, S. H. (2006) The μO-conotoxin MrVIA inhibits voltage-gated sodium channels by associating with domain-3, *FEBS Lett. 580*, 1360−4.
35. Safo, P., Rosenbaum, T., Shcherbatko, A., Choi, D., Han, E., Toledo-Aral, J., Olivera, B. M., Brehm, P., and Mandel, G. (2000) Distinction among neuronal subtypes of voltage-activated sodium channels by μ-conotoxin PIIIA, *J. Neurosci. 20*, 76−80.
36. Akopian, A. N., Souslova, V., England, S., Okuse, K., Ogata, N., Ure, J., Smith, A., Kerr, B. J., McMahon, S. B., Boyce, S., Hill, R., Stanfa, L. C., Dickenson, A. H., and Wood, J. N. (1999) The tetrodotoxin-resistant sodium channel SNS has a specialized function in pain pathways, *Nat. Neurosci. 2*, 541−8.
37. Lyu, Y. S., Park, S. K., Chung, K., and Chung, J. M. (2000) Low dose of tetrodotoxin reduces neuropathic pain behaviors in an animal model, *Brain Res. 871*, 98−103.
38. Gold, M. S., Weinreich, D., Kim, C. S., Wang, R., Treanor, J., Porreca, F., and Lai, J. (2003) Redistribution of $Na_V1.8$ in uninjured axons enables neuropathic pain, *J. Neurosci. 23*, 158−66.

39. Gissen, A. J., Covino, B. G., and Gregus, J. (1982) Differential sensitivity of fast and slow fibers in mammalian nerve. III. Effect of etidocaine and bupivacaine on fast/slow fibers, *Anesth. Analg. 61*, 570−5.
40. Miljanich, G. P. (2004) Ziconotide: Neuronal calcium channel blocker for treating severe chronic pain, *Curr. Med. Chem. 11*, 3029−40.
41. McIntosh, J. M., Corpuz, G. P., Layer, R. T., Garrett, J. E., Wagstaff, J. D., Bulaj, G., Vyazovkina, A., Yoshikami, D., Cruz, L. J., and Olivera, B. M. (2000) Isolation and characerization of a novel *Conus* peptide with apparent antinociceptive activity, *J. Biol. Chem. 275*, 32391−7.
42. Sharpe, I. A., Gehrmann, J., Loughnan, M. L., Thomas, L., Adams, D. A., Atkins, A., Palant, E., Craik, D. J., Adams, D. J., Alewood, P. F., and Lewis, R. J. (2001) Two new classes of conopeptides inhibit the α1-adrenoceptor and noradrenaline transporter, *Nat. Neurosci. 4*, 902−7.
43. Balaji, R. A., Ohtake, A., Sato, K., Gopalakrishnakone, P., Kini, R. M., Seow, K. T., and Bay, B. H. (2000) λ-Conotoxins, a new family of conotoxins with unique disulfide pattern and protein folding. Isolation and characterization from the venom of *Conus marmoreus*, *J. Biol. Chem. 275*, 39516−22.
44. Sandall, D. W., Satkunanathan, N., Keays, D. A., Polidano, M. A., Liping, X., Pham, V., Down, J. G., Khalil, Z., Livett, B. G., and Gayler, K. R. (2003) A novel α-conotoxin identified by gene sequencing is active in suppressing the vascular response to selective stimulation of sensory nerves in vivo, *Biochemistry 42*, 6904−11.
45. Lang, P. M., Burgstahler, R., Haberberger, R. V., Sippel, W., and Grafe, P. (2005) A conus peptide blocks nicotinic receptors of unmyelinated axons in human nerves, *NeuroReport 16*, 479−83.
46. Craig, A. G., Norberg, T., Griffin, D., Hoeger, C., Akhtar, M., Schmidt, K., Low, W., Dykert, J., Richelson, E., Navarro, V., Macella, J., Watkins, M., Hillyard, D., Imperial, J., Cruz, L. J., and Olivera, B. M. (1999) Contulakin-G, an O-glycosylated invertebrate neurotensin, *J. Biol. Chem. 274*, 13752−9.
47. Malmberg, A. B., Gilbert, H., McCabe, R. T., and Basbaum, A. I. (2003) Powerful antinociceptive effects of the cone snail venom-derived subtype-selective NMDA receptor antagonists conantokins G and T, *Pain 101*, 109−16.

BI060159+